# Synthesis and Luminescent Properties of Strong Blue Light-Emitting Al$_2$O$_3$/ZnO Nanocables

Chi-Sheng Hsiao,[a] Wan-Lin Kuo,[a] San-Yuan Chen,[a,z] Ji-Lin Shen,[b] Chin-Ching Lin,[c] and Syh-Yuh Cheng[c]

[a]*Department of Materials Sciences and Engineering, National Chiao Tung University, Hsinchu, Taiwan*
[b]*Physics Department, Chung Yuan Christian University, Chung-Li, Taiwan*
[c]*Materials Research Laboratories, Industrial Technology Research Institution, Chutung, Taiwan*

Photoelectronic characteristics are investigated in well-aligned aluminum-coated ZnO nanorods (Al$_2$O$_3$/ZnO nanocables) grown on Si substrates buffered with ZnO film at a low temperature. Photoluminescence measurement indicates that a strong blue emission peak at $\sim$450 nm appears at 400 and 600°C in O$_2$ and N$_2$ atmospheres, respectively. A 30× enhancement of the relative intensity ratio of blue emission ($I_B$) to ultraviolet emission ($I_{UV}$) has been observed for the Al$_2$O$_3$/ZnO nanocables. High-resolution transmission electron microscopy and X-ray photoelectron spectroscopy analyses reveal that the origin of the strong blue emission can be attributed to the structure transition and cleavage of the oxygen–hydrogen bond (OH) of the Al$_2$O$_3$/ZnO nanocable, which leads to the formation of singly ionized oxygen vacancies (Al–O$^\bullet$).
© 2008 The Electrochemical Society. [DOI: 10.1149/1.2890289] All rights reserved.

Al$_2$O$_3$ has been used for capacitor dielectrics and gate oxides in memory devices due to its high dielectric constant, very low permeability, and high thermal conductivity.[1] However, the photoluminescence (PL) property of alumina film or nanoparticles has not been studied in detail. Yoldas et al. studied alumina–silica powders and stated that the presence of pentahedrally coordinated aluminum appears to be strongly correlated with the occurrence of PL.[2] Suga et al. studied alumina gel from an inorganic salt and alkoxide, and mentioned that the PL is closely related to oxygen defects and the development of the Al$^V$ site.[3] However, no data exist for determining the dependence of the properties of a defect center on the structure of its coordinate sites and the presence of luminescence. Recently, Li et al. reported that a broad band located around 422 nm could be detected from nanosized γ-Al$_2$O$_3$ powder.[4] It is suggested that the produced defect level could induce γ-Al$_2$O$_3$ nanopowder to emit blue PL bands. However, most of those studies have been focused on nanopowders or gel films. In past years, ZnO/Al$_2$O$_3$ core/shell nanofibers have been prepared from the Al$_2$O$_3$ deposition of ZnO nanowires with an atomic layer deposition technique, but no PL properties have been reported.[5] These findings indicate that so far, the PL property of nanoscale alumina film has not been investigated. In addition, our previous study found that, when an alumina film is deposited on a ZnO-coated silicon substrate by a wet chemical process, the alumina film not only emits blue, but the blue emission can also be much enhanced compared to that of coatings on pure silicon. This indicates that ZnO plays an important role in the PL properties of nanosized alumina films.

Wet chemical approaches are widely used for the fabrication of large oriented arrays of ZnO nanorods on Si or polymer organic substrates. Furthermore, zinc oxide is an important photoelectronic material because of its wide direct bandgap of 3.37 eV and a relatively large exciton binding energy of 60 meV,[6] which makes ZnO a promising material for light-emitting diodes or diode lasers. In addition, depending on the processing methods, a variety of defects can be easily generated from nanostructured ZnO. Therefore, it is possible to develop the Al$_2$O$_3$/ZnO nanostructure into white phosphor if the blue emission from alumina can be incorporated into the ZnO nanostructure. So far, to the best of our knowledge, there have been no further systematic investigations on the light-emitting properties of alumina-coated ZnO nanorods grown in aqueous solutions at lower temperatures. Furthermore, it has been challenging to develop Al$_2$O$_3$/ZnO or ZnO-based nanostructures with a strong light emission by simple wet chemical processing. Therefore, in this work, a simple method of combining the aqueous solution process

with a thermal treatment is proposed to develop Al$_2$O$_3$/ZnO nanocables with a strong blue emission. The structure and optical properties of the nanocables also will be discussed. In addition, the application of this advanced structure to modify luminescent properties demonstrates a way to develop nanostructures for optoelectronic applications.

## Experimental

Previous experiments have shown that highly arrayed ZnO nanorods can be developed on ZnO film-coated Si (ZnO$_f$/Si) substrates.[7] Following the sol–gel porous alumina templating method proposed by Martin et al.,[8] 5 M ammonia was added to an aqueous alumina nitrate solution (0.4 M) at room temperature. After the hydrated precipitate was formed, it was centrifugally separated and washed several times with distilled water. The precipitates were then peptized with nitric acid to obtain a translucent, homogeneous, and stable sol. After that, the ZnO nanorods were exposed to surface modification by oxygen plasma treatment, and were subsequently immersed in the precursor sol of Al$^{+3}$ to grow an alumina shell on the ZnO nanorods at 80°C for 1 h. The thickness of the alumina shell on the ZnO nanorods can be modulated by controlling the reaction parameters. After washing with distilled water, rapid thermal annealing was performed for aluminum sol-coated ZnO nanorods at 200–600°C in nitrogen and oxygen atmospheres. Microstructure observation of Al$_2$O$_3$/ZnO nanocables was performed by a transmission electron microscope (TEM, JEOL 2010) operated at 200 keV. Room-temperature PL measurement was performed on the nanorod samples, which were excited by a 325 nm He–Cd laser with an excitation power of 25 mW. The emitted luminescence light was collected through a 0.32 m spectrometer with a charge-coupled device detector. The focused spot size of the He–Cd laser was estimated to be about 200 μm in diameter. X-ray photoelectron spectroscopy (XPS) was used to evaluate the Al–O chemical binding states. The $^{27}$Al magic angle spinning nuclear magnetic resonance (MAS NMR) was used to examine the chemical shift of alumina-coated ZnO nanrods scraped from the Si substrate using a Bruker Dsx400wc NMR spectrometer. The XPS analyses were performed on a Kratos AXIS Ultra with a monochromatic Mg X-ray source at 150 W.

## Results and Discussion

Figure 1a shows the scanning electron microscope (SEM) surface image of the arrayed as-synthesized Al$_2$O$_3$/ZnO nanocables grown vertically on ZnO$_f$/Si substrates. It was found that the nanorods have a well-defined hexagonal plane with a diameter of approximately 20–30 nm. Further analysis on as-synthesized Al$_2$O$_3$/ZnO nanocables is shown in the TEM image of Fig. 1b,

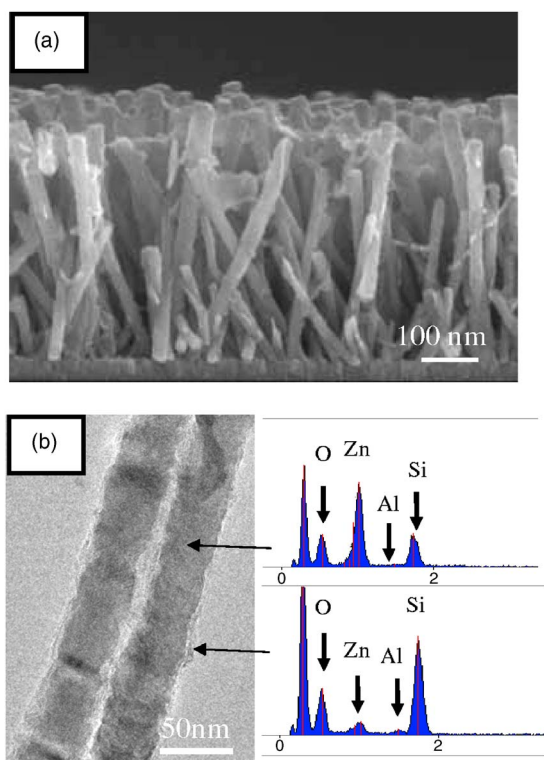z E-mail: sanyuanchen@mail.nctu.edu.tw

**Figure 1.** (Color online) SEM images of (a) side view of ZnO nanorods. (b) TEM image and EDS analysis of $Al_2O_3$/ZnO nanocables.

indicating that alumina was conformally deposited on the ZnO nanorods and that the nanorods remained in their original shape. Energy-dispersive spectroscopy (EDS) analysis further confirmed that only strong Zn and O signals without Al were identified in the core nanorods, but that a weak peak corresponding to Al could be detected from the shell, indicating that an alumina shell was formed on the ZnO nanorods at low temperature.

The high-resolution (HR) TEM image in Fig. 2a illustrates that alumina was conformally deposited on the ZnO nanorods to become a core/shell $Al_2O_3$/ZnO nanocable structure. From the selected area electron diffraction in the inset of Fig. 2a, two diffraction patterns (rings and spot patterns) are observed. The spot pattern is from the single-crystal ZnO structure, while the ring pattern can be attributed to an amorphous alumina structure that may be a pseudo-
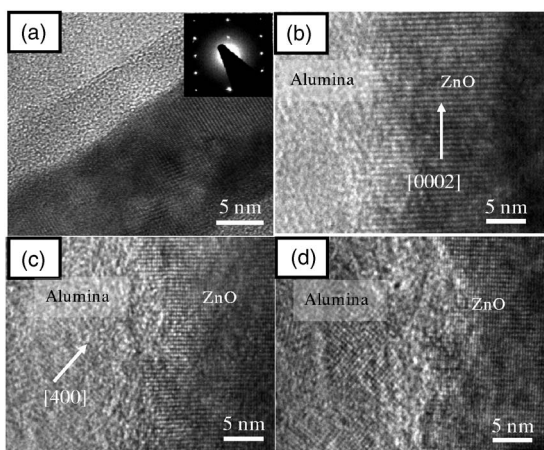


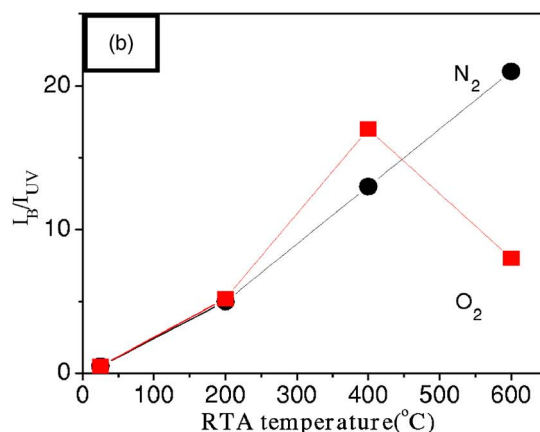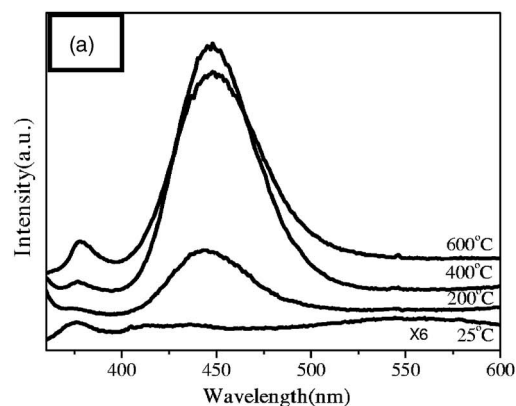**Figure 2.** HRTEM of $Al_2O_3$/ZnO nanocables (a) as-synthesized and annealed at (b) 200°C; (c) 400°C and (d) 600°C in oxygen ambient.



**Figure 3.** (Color online) (a) Room-temperature PL spectra of $Al_2O_3$/ZnO nanocables after rapid thermal anneal at various temperatures in $O_2$ atmosphere. (b) The relative PL ratios ($I_B/I_{UV}$) of blue emission to UV emission on annealing temperature as a function of $O_2$ and $N_2$ atmospheres.

boehmite phase developed in aqueous solution according to the report of Ishizaka.[9] Upon annealing at 200°C, a short-range ordered structure seems to develop in the alumina shell, as shown in the HRTEM image of Fig. 2b. It is believed that rapid thermal treatment in an $O_2$ atmosphere is favorable for the cleavage of the oxygen–hydrogen bond (OH), causing the departure of H ions from the pseudoboehmite and initiating the occurrence of the phase transformation of amorphous pseudoboehmite into a γ-phase alumina structure. This structure can be thought of as a cubic spinel, with some suggestion of a tetragonal (tetrahedrally coordinated aluminum) distortion in boehmite-derived γ-$Al_2O_3$ in the $I4_1/amd$ space group.[10] When annealed at 400°C in an $O_2$ atmosphere, a long-range ordered structure can be clearly observed from the HRTEM image in Fig. 2c. According to the calculation of the lattice fringe (about 0.2 nm), it was indexed as a (400) plane, indicating a γ-phase alumina structure ($d = 0.198$ nm). This suggests that with increasing the temperature to 400°C in an $O_2$ atmosphere, the γ-phase was developed in the alumina shell. As annealed at 600°C, two kinds of lattice fringes are clearly observed for annealed $Al_2O_3$/ZnO nanocables as shown in Fig. 2d, indicating that, in addition to single-crystalline ZnO nanorods, a crystalline γ-alumina structure has been completely formed in the alumina shell at 600°C.

Figure 3a shows the room-temperature PL property of $Al_2O_3$/ZnO nanocables at different temperatures. Three important emission peaks can be observed from the PL spectrum of as-synthesized alumina-coated ZnO nanocables. Both ultraviolet (UV) emission (378 nm) and green–yellow (visible) emission (525–575 nm) bands are attributed to ZnO nanorods, and the other broad blue emission (425–475 nm) is possibly from the alumina shell. The near bandedge (UV emission) is generally attributed to free-exciton re-

combination, but the green–yellow emission is produced from the oxygen defect of the pure ZnO nanorods fabricated by chemical solution methods.[11] In fact, it was found that the UV emission intensity of the as-grown nanocables increases with the annealing temperature at 200–600°C in an oxygen ambient, but the visible emission in postannealed samples tends to disappear, suggesting that the native defects can be reduced by postannealing treatment as shown in Fig. 3a. It was noted that when the $Al_2O_3$/ZnO nanocables are annealed at 200°C in an $O_2$ atmosphere, an obvious blue emission at around 450 nm, which was primarily contributed from the alumina shell, can be clearly identified. According to the report of Lippens et al.[12] and TEM analysis (Fig. 1), an increase of the annealing temperature may cause the cleavage of the oxygen–hydrogen bond (OH) in pseudoboehmite structure, and consequently, both Al–O–O• and Al–O• defects would probably be produced in the alumina shell and vary with annealing temperature and atmospheres. At a lower temperature, i.e., 200°C, Al–O–O• defects are much more easily generated than Al–O•. However, according to Ishizaka's report, the distance between the aluminum atom and the electron spin in Al–O–O• is long enough to neglect the hyperfine interaction with Al, indicating that Al–O–O• would not be a luminescent center.[13] With the increase of the annealing temperature, the OH bond in the pseudoboehmite structure tends to be broken and Al–O• would be formed during the phase transformation from the pseudoboehmite phase (octahedrally coordinated structure) to the γ-phase aluminum oxide (tetrahedrally coordinated structure), favoring pentahedrally coordinated aluminum and the occurrence of singly ionized oxygen vacancies which are regarded as the $F^+$ center.[14]

With increasing the temperature to 400°C, dehydration proceeds and the structure evolves through a series of disordered states during the phase transformation from pseudoboehmite to γ-phase as demonstrated in Fig. 2c. In this condition, pentahedrally coordinated aluminum is easily formed, indicating that more singly ionized oxygen vacancies ($F^+$ center) defects can be generated. Therefore, a strong blue emission can be observed. At a higher temperature, i.e., 600°C, although the positions of the blue emission remain unchanged, it is found that the peak intensity is weakened compared to the sample annealed at 400°C. This indicates that the defect density of the main defects ($F^+$ centers) responsible for the blue emission is decreased with increasing the annealing temperature up to 600°C. Consequently, the density of the $F^+$ centers is reduced due to compensation in the $O_2$ atmosphere.

As reported, ZnO material usually generates a strong UV emission.[15] However, it can be seen in the figure that UV emission decreases while blue light emission increases. It can be inferred that UV emission from the ZnO band-edge recombination can excite the blue light of aluminum oxide. This may result in different intensity ratios of blue light to UV in the PL spectra. To further investigate the effect of heat treatment on the $F^+$ centers and pentahedrally coordinated aluminum, the as-synthesized $Al_2O_3$/ZnO nanocable samples were subjected to annealing at different temperatures in $N_2$ and $O_2$ atmospheres. The relative PL ratios ($I_B/I_{UV}$) of blue emission to UV emission on annealing temperature as a function of $O_2$ and $N_2$ atmospheres is presented in Fig. 3b. It is observed that the strongest blue emission of the nanocables appears at 600°C in a nitrogen ambient instead of 400°C in an oxygen atmosphere. Furthermore, the blue emission of postannealed $Al_2O_3$/ZnO nanocables is dominated not only by the annealing temperature but also the annealing atmosphere because the PL emission is very sensitive to defect type.[16] As dehydration proceeds, the structure evolves through a series of disordered states, probably from octahedral to pentahedral and then tetrahedral. Ishizaka et al. reported that the luminescence is maximized for alumina treated at 600°C, at which temperature γ-alumina is formed.[13] Yoldas et al. studied calcium aluminate glass and suggested that the pentahedrally coordinated aluminum ($Al^V$) may be strongly correlated with the occurrence of luminescence.[2] Therefore, $^{27}Al$ NMR analysis was performed to characterize such complexes.[17] Figure 4 shows the $^{27}Al$ MAS NMR
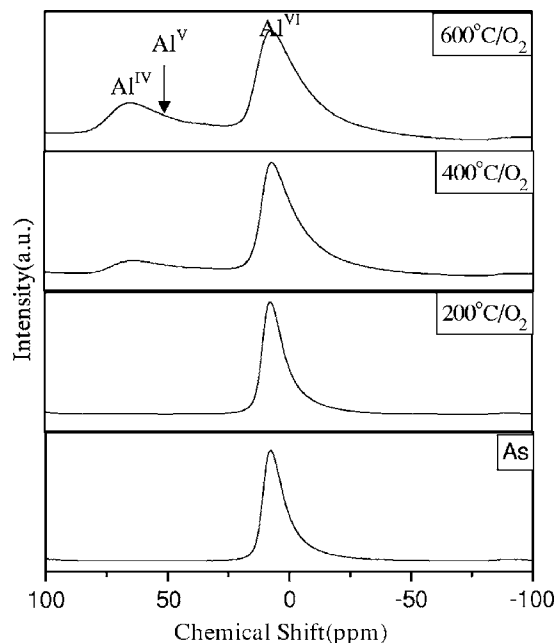


**Figure 4.** $^{27}Al$ MAS NMR spectra for the alumina-coated ZnO nanorods annealed in $O_2$.

spectra of these samples as a function of the annealing temperature. Besides the resonance lines attributable to tetrahedrally ($Al^{IV}$) and octahedrally ($Al^{VI}$) coordinated aluminum, a line corresponding to pentahedrally ($Al^V$) coordinated aluminum has also been observed. It was found that the concentration of pentahedrally coordinated ($Al^V$) aluminum is dependent on the thermochemical environment within the samples. Furthermore, the $Al^V$ signal increases with the firing temperature, reaches a maximum intensity at about 600°C, and then decreases at a higher temperature in both $O_2$ and $N_2$ annealing atmospheres. When comparing Fig. 3b, it was noted that, although the concentration of pentahedrally coordinated aluminum is higher at 600°C, the relative peak intensity ($I_B/I_{UV}$) of the $O_2$-annealed nanocables is decreased. This may imply that with the increase of annealing temperature, the OH bond in the pseudoboehmite structure tends to be broken and produce more pentahedrally coordinated aluminum and singly ionized oxygen vacancies ($F^+$). However, the $F^+$ centers would be compensated in the case of annealing in oxygen at a higher annealing temperature, i.e., 600°C. Therefore, in this condition $F^+$ centers decrease, but the pentahedrally coordinated aluminum still exists as indicated from the NMR result.

Because the equilibrium structure during the transformation of boehmite to γ-alumina phase is determined by the number of the OH groups,[18] the surface composition of $Al_2O_3$/ZnO nanocables was further examined by XPS for samples annealed at 400°C in $N_2$ and $O_2$ atmospheres as shown in Fig. 5. XPS spectra of Al 2p in annealed $Al_2O_3$/ZnO nanocables are shown in Fig. 5a. The peak position for the samples with nearly stoichiometric composition annealed in a $N_2$ atmosphere is located at a binding energy of 74.3 eV, indicating that the Al–O binding state is dominated by the boehmite/γ-alumina phase. In contrast, the Al 2p position of the samples annealed in an $O_2$ atmosphere is located at a binding energy of 74.6 eV, indicating that γ-alumina is easily formed for the sample treated in $O_2$ gas. The asymmetric spectrum of O 1s in Fig. 5b and c contains three peaks at 529.6, 530.8, and (broadly) 532.6 eV. The peaks around 529.6 and 530.8 eV can be assigned to $O^{2-}$ ions in the Zn–O bonds and Al–O bonds, respectively. The peak related to the highest binding energy around 532.6 eV is attributed to OH bonds. As a result, a strong OH–bond peak was observed in a $N_2$ atmo-
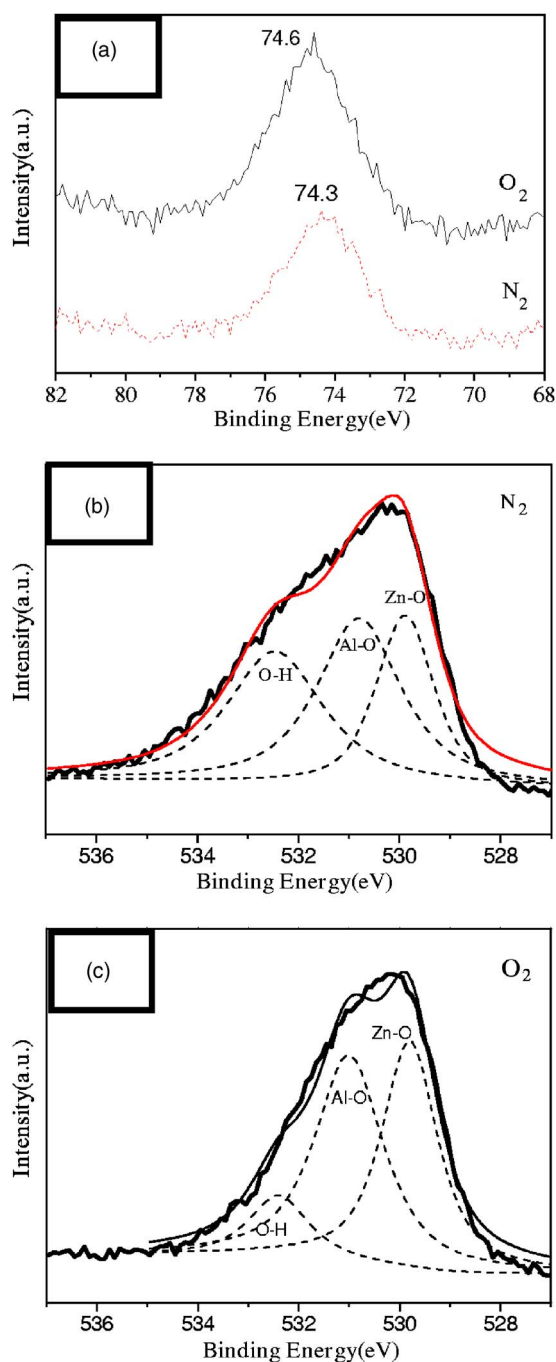
**Figure 5.** (Color online) XPS spectra for the Al$_2$O$_3$/ZnO nanocables of (a) Al 2p and O 1s annealed in (b) N$_2$ and (c) O$_2$ at 400°C.

sphere compared to that in an O$_2$ atmosphere. This again demonstrates that more F$^+$ centers are produced by the rapid thermal treatment of 400°C in an O$_2$ atmosphere, resulting in a stronger blue emission.

However, with a further increase of the annealing temperature up to 600°C, it was found that the $I_B/I_{UV}$ decreases in an O$_2$ atmosphere but increases in a N$_2$ atmosphere. The F$^+$ centers would be diminished due to compensation in O$_2$ atmosphere. In contrast, $I_B/I_{UV}$ continuously increases and reaches the maximum intensity at 600°C in a N$_2$ atmosphere. Therefore, the relative $I_B/I_{UV}$ intensity of the Al$_2$O$_3$/ZnO nanocables annealed in a N$_2$ atmosphere is stronger than that in an O$_2$ atmosphere at 600°C, indicating the difficulty of compensating F$^+$ centers in a nitrogen ambient. Therefore, in this work, it can be concluded that the blue emission is primarily dominated by F$^+$ centers that are accompanied by the occurrence of pentahedrally coordinated aluminum during the phase evolution of the Al$_2$O$_3$ shell on the ZnO nanorods.

## Conclusion

In summary, we have developed well-aligned arrays of Al$_2$O$_3$/ZnO nanocables on ZnO$_f$/Si substrates buffered with a ZnO film by combining a simple chemical solution with a low-temperature treatment. The PL measurement indicates that a strong blue emission peak at ~450 nm appears at 400 and 600°C in O$_2$ and N$_2$ atmospheres, respectively. The phenomenon is strongly related to OH bond cleavage and a phase transition from amorphous to γ-phase alumina, as evidenced by XPS and NMR analyses. The results provide an effective method for constructing nanostructures with a strong blue light emission.

## References

1. E. P. Gusev, M. Copel, E. Cartier, I. J. R. Baumvol, C. Krug, and M. A. Gribelyuk, *Appl. Phys. Lett.*, **76**, 176 (2000).
2. B. E. Yoldas, *J. Non-Cryst. Solids*, **147–148**, 614 (1992).
3. Y. Kurokawa, T. Suga, S. Nakata, T. Ikoma, and S. Tero-Kubota, *J. Mater. Sci. Lett.*, **17**, 275 (1998).
4. Z. Q. Yu, D. Chang, and C. Li, *J. Mater. Res.*, **16**, 1890 (2001).
5. J. Hwang, B. Min, J. S. Lee, K. Keem, K. Cho, M. Y. Sung, M. S. Lee, and S. Kim, *Adv. Mater.*, **16**, 422 (2004).
6. D. B. Laks, *Appl. Phys. Lett.*, **63**, 1375 (1993).
7. S. C. Liou, C. S. Hsiao, and S. Y. Chen, *J. Cryst. Growth*, **274**, 438 (2005).
8. B. Cheng and E. T. Samulski, *J. Mater. Chem.*, **11**, 2901 (2001).
9. T. Ishizaka and S. T. Kubota, *J. Phys. Chem. Solids*, **64**, 801 (2003).
10. G. Paglia, S. Božin, and J. L. Billinge, *Chem. Mater.*, **18**, 3242 (2006).
11. D. Li, Y. H. Leung, A. B. Djurisic, Z. T. Liu, M. H. Xie, S. L. Shi, S. J. Xu, and W. K. Chan, *Appl. Phys. Lett.*, **85**, 1601 (2004).
12. B. C. Lippens and J. H. de Boer, *Acta Crystallogr.*, **17**, 1312 (1964).
13. T. Ishizaka and Y. Kurokawa, *J. Appl. Phys.*, **90**, 2257 (2001).
14. Y. Du, W. L. Cai, C. M. Mo, J. Chen, L. D. Zhang, and X. G. Zhu, *Appl. Phys. Lett.*, **74**, 2951 (1999).
15. N. E. Hsu, W. K. Hung, and Y. F. Chen, *J. Appl. Phys.*, **96**, 4671 (2004).
16. X. L. Wu, G. G. Siu, C. L. Fu, and H. C. Ong, *Appl. Phys. Lett.*, **78**, 2285 (2001).
17. T. Ishizaka and S. T. Kubota, *J. Phys. Chem. Solids*, **64**, 801 (2003).
18. M. Nguefack, A. F. Popa, S. Rossignol, and C. Kappenstein, *Phys. Chem. Chem. Phys.*, **5**, 4279 (2003).